CONSTRAINED TOPOLOGY OPTIMIZATION FOR LAMINAR AND TURBULENT FLOWS, INCLUDING HEAT TRANSFER

E.M. Papoutsis-Kiachagias*,
E.A. Kontoleontos,
A.S. Zymaris,
D.I. Papadimitriou,
K.C. Giannakoglou
National Technical University of Athens,
School of Mechanical Engineering,
Parallel CFD & Optimization Unit,
P.O. Box 64069, Athens 157 10, Greece,
Email: kgianna@central.ntua.gr

Abstract. The continuous adjoint approach to topology optimization in incompressible, laminar and turbulent ducted flows, is presented. An unknown variable porosity field, to be determined during the optimization, is the means to define the optimal topology configuration. Regarding turbulent flows, these are handled using the Spalart-Allmaras turbulence model and the proposed adjoint approach is exact, i.e. includes the adjoint to the turbulence model equation, too. In design problems of ducts (manifolds) with many outlets, constraints on the flow rate at each outlet boundary are imposed. Compared to other published works on the use of adjoint methods in topology optimization and apart from the exact differentiation of the turbulence model, the present paper extends the porosity-based method to also account for flow problems and objective functions including heat transfer. The proposed method is applied to three ducted flow problems.

Key words: topology optimization, continuous adjoint, laminar and turbulent flows, heat transfer, constrained optimization

1 INTRODUCTION

More than 20 years ago, the notion of topology optimization was introduced in structrural mechanics[1], by formulating and numerically solving equations in terms of material density in order to identify areas in which material should be added so as to increase structural stiffness. The idea was, then, adapted to CFD problems, for either Stokes[2] or laminar[3] flows, by introducing a variable porosity field. In fluids, the optimization aims at computing the porosity field over an extended (porous media) domain that minimizes the objective function; based on the local porosity values, domain areas corresponding to the fluid flow are identified, whereas the remaining areas define the surrounding solid bodies. The optimal solid walls to be designed correspond to the interfaces between the two aforementioned areas. In Fig. 1, the concept of the topology optimization method in fluid mechanics is presented.
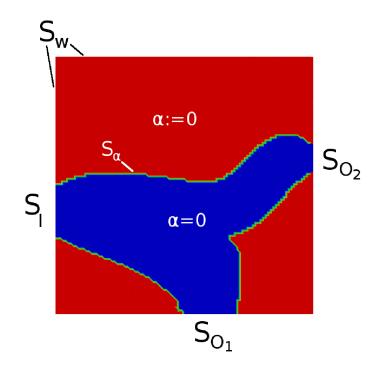
Figure 1: Schematical representation of the porous media domain and its boundaries. S_I is the predefined inlet to the porous media domain, S_{O_l}, $l = 1, L$ are its outlets and S_W are the solid wall boundaries of the porous media domain. Topology optimization algorithms seek the optimal distribution of the variable porosity, in order to minimize the objective function under consideration. Upon completion of the optimization, red/bright areas with a non-zero porosity value ($\alpha \neq 0$) correspond to the 'solid body' domain (practically, with zero flow within those regions). Blue/dark areas indicate the flow passage ($\alpha = 0$). The new 'solid wall' boundary, S_α, is the interface between the two aforementioned areas (green/white line).

The adjoint approach for solving topology optimization problems in laminar flows has been presented just a few years ago[4]. The present work relies on that paper, as far as the introduction of porosity into the flow equations is concerned (with the introduction of extra porosity–dependent terms into the energy and turbulence model equations, should these have to be solved too) as well as to a recent paper by some of the present authors[5], where the exact continuous adjoint method for turbulent flows was presented. The latter was exclusively dealing with shape optimization and the present paper is, from a different viewpoint, its extension to topology optimization.

In the present paper, applications of the topology optimization method for the design of ducts/manifolds in incompressible, laminar and turbulent flows are presented. The continuous adjoint method will be used to compute the required sensitivity derivatives and, through them, drive a gradient–based method, leading to the optimal porosity field. As mentioned before, in turbulent cases, the adjoint equation to the Spalart– Allmaras turbulence model is, also, solved. Finally, in the topology optimization of manifolds with more that one outlets, constraints on the volume flow rates from each one of the outlet boundaries should often be imposed; to compute the gradient of the constraint functions, the continuous adjoint method was extended accordingly. In one of the topology optimization problems examined, the objective function takes into account the exchanged amount of heat between the fluid and its surrounding solid; in this problem, the energy equation must be also solved.

2 TOPOLOGY OPTIMIZATION IN TURBULENT INCOMPRESSIBLE FLOWS WITH HEAT TRANSFER

In the most general case, the state (or primal) problem is governed by the steady–state Navier–Stokes equations for incompressible fluid flows with heat transfer, in which terms depending on the porosity variable α have been introduced. The state equations are $R_p = 0, \ R_{v_i} = 0, \ R_T = 0$, where

$$R_p \ = \ \frac{\partial v_j}{\partial x_j} \tag{1}$$

$$R_{v_i} \ = \ v_j \frac{\partial v_i}{\partial x_j} + \frac{\partial p}{\partial x_i} - \frac{\partial}{\partial x_j}\left[(\nu + \nu_t)\left(\frac{\partial v_i}{\partial x_j} + \frac{\partial v_j}{\partial x_i} \right)\right] + \alpha v_i \tag{2}$$

$$R_T \ = \ v_j \frac{\partial T}{\partial x_j} - \frac{\partial}{\partial x_j}\left[\left(\frac{\nu}{Pr} + \frac{\nu_t}{Pr_t}\right)\frac{\partial T}{\partial x_j}\right] + \alpha\left(T - T_{wall}\right) \tag{3}$$

where p, v_i, T denote the static pressure, the velocity components and the static temperature, respectively. Also ν, ν_t are the bulk and turbulent viscosities, Pr, Pr_t are the laminar and turbulent Prandtl numbers and T_{wall} is the constant–known temperature along the solid wall surrounding the flow.

In turbulent flows, based on the Spalart–Allmaras turbulence model[6], the turbulent viscosity is given by $\nu_t = \tilde{\nu} f_{v_1}$, where $\tilde{\nu}$ is the solution variable in the additional state equation, $R_{\tilde{\nu}} = 0$. The turbulence model equation, in which a term depending on α is also introduced, reads

$$R_{\tilde{\nu}} = v_j \frac{\partial \tilde{\nu}}{\partial x_j} - \frac{\partial}{\partial x_j}\left[\left(\nu + \frac{\tilde{\nu}}{\sigma}\right)\frac{\partial \tilde{\nu}}{\partial x_j}\right] - \frac{c_{b_2}}{\sigma}\left(\frac{\partial \tilde{\nu}}{\partial x_j}\right)^2 - \tilde{\nu} P\left(\tilde{\nu}\right) + \tilde{\nu} D\left(\tilde{\nu}\right) + \alpha\tilde{\nu} \tag{4}$$

The production $P(\tilde{\nu})$ and destruction $D(\tilde{\nu})$ terms as well as f_{v_1}, c_{b_2}, σ are as in[6].

The mean-flow equations are solved in a segregated manner by employing the SIMPLE algorithm[7] and the heat transfer and turbulence equations are solved decoupled from them.

Eqs. 1 to 4 are numerically solved on an extended (porous media) domain, with fixed inlets and outlets along its boundary. For this purpose, unstructured grids, with appropriate stretching close to the boundaries, are generated. Over the grid nodes with zero porosity, terms αv_i, $\alpha\left(T - T_{wall}\right)$ and $\alpha\tilde{\nu}$ are eliminated and these nodes belong to the free flow passage since the local state variables satisfy the flow equations. In contrast, nodes with non–zero local porosity yield zero velocity (so as to eliminate term αv_i in eq. 2) and temperature equal to T_{wall} (so as to eliminate term $\alpha\left(T - T_{wall}\right)$ in eq. 3) and correspond to the solid bodies surrounding the flow. Over the same nodes, based on eq. 4, the turbulence model variable is zero, as well.

Given that the incoming flow rate is determined by integrating the imposed inlet velocity profile, constraints on the flow rate exiting from each one of the user–defined outlet boundaries can optionally be imposed.

In the general case (i.e. in a constrained optimization problem), the user–defined objective function F is augmented by the state equations, $R_p = 0, R_{v_i} = 0, R_T = 0, R_{\tilde{\nu}} = 0$, as well as by the constraint c, forming the augmented objective function, F_{aug}

$$F_{aug} = F + \int_\Omega q R_p d\Omega + \int_\Omega u_i R_{v_i} d\Omega + \int_\Omega T_a R_T d\Omega + \int_\Omega \tilde{\nu}_a R_{\tilde{\nu}} d\Omega + \omega_c c \tag{5}$$

where $q, u_i, T_a, \tilde{\nu}_a$ denote the adjoint pressure, velocities, temperature and turbulence model variables and ω_c denotes a user-defined weight for the constraint function, respectively.

For the third case examined in this paper, where L outlets are defined, c is given by

$$c = \frac{1}{2} \sum_{l=1}^{L} (\Delta m_l)^2 = 0 \tag{6}$$

where Δm_l stands for

$$\Delta m_l = \int_{S_{O_l}} v_i n_i dS + r_l \int_{S_I} v_i n_i dS \tag{7}$$

and S_{O_l}, r_l stand for the l-th outlet boundary of the domain and the desirable volume flow rate ratio, with respect to the overall incoming flow rate (from S_I); n_i is the outward unit normal vector. It is $\sum_{l=1}^{L} r_l = 1$.

In general, the global variation (symbol δ) of any quantity Φ with respect to a design variable b, is expressed as the sum of direct (symbol ∂) and grid-dependent variations, namely

$$\frac{\delta \Phi}{\delta b} = \frac{\partial \Phi}{\partial b} + \frac{\partial \Phi}{\partial x_k} \frac{\partial x_k}{\partial b} \tag{8}$$

In topology optimization problems, the boundaries of the porous media domain remain unchanged, so $\frac{\partial x_k}{\partial \alpha} = 0$ and symbols δ and ∂ can be used indiscriminatelly $\left(\frac{\delta \Phi}{\delta \alpha} = \frac{\partial \Phi}{\partial \alpha} \right)$.

Taking that into account, the variation of F_{aug} with respect to the porosity variable is expressed as

$$\frac{\delta F_{aug}}{\delta \alpha} = \frac{\delta F}{\delta \alpha} + \int_{\Omega} q \frac{\partial R_p}{\partial \alpha} d\Omega + \int_{\Omega} u_i \frac{\partial R_{v_i}}{\partial \alpha} d\Omega + \int_{\Omega} T_a \frac{\partial R_T}{\partial \alpha} d\Omega + \int_{\Omega} \tilde{\nu}_a \frac{\partial R_{\tilde{\nu}}}{\partial \alpha} d\Omega + \omega_c \frac{\partial c}{\partial \alpha} \tag{9}$$

The last term in eq. 9 stands for the effect of the constraint on the topology optimization. Term $\frac{\partial c}{\partial \alpha}$ can be written as

$$\frac{\partial c}{\partial \alpha} = \sum_{l=1}^{L} \Delta m_l \int_{S_{O_l}} \frac{\partial v_i}{\partial \alpha} n_i dS \tag{10}$$

since v_i are fixed along S_I.

The development of the field integrals of eq. 9, by using the Gauss divergence theorem, leads finally to the following expression:

$$
\begin{aligned}
\frac{\delta F_{aug}}{\delta \alpha} &= \frac{\delta F}{\delta \alpha} + \int_{\Omega} R_q \frac{\partial p}{\partial \alpha} d\Omega + \int_{\Omega} R_{u_i} \frac{\partial v_i}{\partial \alpha} d\Omega + \int_{\Omega} R_{\tilde{\nu}_a} \frac{\partial \tilde{\nu}}{\partial \alpha} d\Omega + \int_{\Omega} R_{T_a} \frac{\partial T}{\partial \alpha} d\Omega \\
&+ \int_{\Omega} v_i u_i d\Omega + \int_{\Omega} \tilde{\nu} \tilde{\nu}_a d\Omega + \int_{\Omega} (T - T_{wall}) T_\alpha d\Omega + \int_{\Omega} \tilde{\nu}_a \tilde{\nu} \mathcal{C}_d(\tilde{\nu}, \vec{v}) \frac{\partial d}{\partial \alpha} d\Omega \\
&+ \int_S \left(u_j n_j + \frac{\partial F}{\partial p} \right) \frac{\partial p}{\partial \alpha} dS + \int_S \mathcal{BC}_{1,i} \frac{\partial v_i}{\partial \alpha} dS + \int_S \mathcal{BC}_2 \frac{\partial \tilde{\nu}}{\partial \alpha} dS + \int_S \mathcal{BC}_3 \frac{\partial T}{\partial \alpha} dS \\
&- \int_S (\nu + \nu_t) \frac{\partial}{\partial \alpha} \left(\frac{\partial v_i}{\partial x_j} + \frac{\partial v_j}{\partial x_i} \right) u_i n_j dS - \int_S \tilde{\nu}_a \left(\nu + \frac{\tilde{\nu}}{\sigma} \right) \frac{\partial}{\partial \alpha} \left(\frac{\partial \tilde{\nu}}{\partial x_j} n_j \right) dS \\
&- \int_S \left(\frac{\nu}{Pr} + \frac{\nu_t}{Pr_t} \right) T_a \frac{\partial}{\partial \alpha} \left(\frac{\partial T}{\partial x_j} n_j \right) dS
\end{aligned}
\tag{11}
$$

where $S = S_I \cup S_O \cup S_W$ (S_I, S_O, S_W the inlet, outlet and wall boundaries of the porous media domain Ω, respectively) and d is the distance from S_α.

Thus, based on eq. 11, the adjoint field equations are derived by eliminating field integrals depending on $\frac{\partial p}{\partial \alpha}$, $\frac{\partial v_i}{\partial \alpha}$, $\frac{\partial \tilde{\nu}}{\partial \alpha}$, $\frac{\partial T}{\partial \alpha}$. The field adjoint to the mean-flow, energy and turbulence equations are given by

$$R_q = 0, \quad R_{u_i} = 0, \quad R_{T_a} = 0, \quad R_{\tilde{\nu}_a} = 0 \tag{12}$$

where

$$R_q = \frac{\partial u_j}{\partial x_j} \tag{13}$$

$$R_{u_i} = -v_j \left(\frac{\partial u_i}{\partial x_j} + \frac{\partial u_j}{\partial x_i} \right) + \frac{\partial q}{\partial x_i} - \frac{\partial}{\partial x_j} \left[(\nu + \nu_t) \left(\frac{\partial u_i}{\partial x_j} + \frac{\partial u_j}{\partial x_i} \right) \right]$$

$$+ \underbrace{\tilde{\nu} \frac{\partial \tilde{\nu}_a}{\partial x_i} + \frac{\partial}{\partial x_k} \left(e_{jki} e_{jmq} \frac{\mathcal{C}_S}{S} \frac{\partial v_q}{\partial x_m} \tilde{\nu} \tilde{\nu}_a \right)}_{termM1} + \underbrace{T \frac{\partial T_a}{\partial x_i}}_{termM2} + \alpha u_i \tag{14}$$

$$R_{T_a} = -v_j \frac{\partial T_a}{\partial x_j} - \frac{\partial}{\partial x_j} \left[\left(\frac{\nu}{Pr} + \frac{\nu_t}{Pr_t} \right) \frac{\partial T_a}{\partial x_j} \right] + \alpha T_a \tag{15}$$

$$R_{\tilde{\nu}_a} = -v_j \frac{\partial \tilde{\nu}_a}{\partial x_j} - \frac{\partial}{\partial x_j} \left[\left(\nu + \frac{\tilde{\nu}}{\sigma} \right) \frac{\partial \tilde{\nu}_a}{\partial x_j} \right] + \frac{1}{\sigma} \frac{\partial \tilde{\nu}_a}{\partial x_j} \frac{\partial \tilde{\nu}}{\partial x_j} + 2 \frac{c_{b2}}{\sigma} \frac{\partial}{\partial x_j} \left(\tilde{\nu}_a \frac{\partial \tilde{\nu}}{\partial x_j} \right) + \tilde{\nu}_a \tilde{\nu} \, \mathcal{C}_{\tilde{\nu}}(\tilde{\nu}, \vec{v})$$

$$+ (-P + D) \tilde{\nu}_a + \frac{\delta \nu_t}{\delta \tilde{\nu}} \frac{\partial u_i}{\partial x_j} \left(\frac{\partial v_i}{\partial x_j} + \frac{\partial v_j}{\partial x_i} \right) + \underbrace{\frac{\delta \nu_t}{\delta \tilde{\nu}} \frac{1}{Pr_t} \frac{\partial T_a}{\partial x_j} \frac{\partial T}{\partial x_j}}_{termT1} + \alpha \tilde{\nu}_a \tag{16}$$

Detailed expressions of terms $\mathcal{C}_S$, $\mathcal{C}_{\tilde{\nu}}$, $\mathcal{C}_d$, S can be found in[5]; e_{jki} is the permutation symbol. In eq. 14, $termM1$ and $termM2$ result from the differentiation of the turbulence model and energy equations respectively, whereas $termT1$ is the contribution of the energy equation's differentiation to the adjoint turbulence model field equation (eq. 16). Whenever the primal turbulence model and/or energy equations are not solved, terms and equations resulting from their differentiation are omitted from the adjoint formulation.

In addition, elimination of boundary integrals which depend on variations of the flow variables in eq. 11 yields the adjoint boundary conditions. These are described below:

The outlet conditions for q and u_i, along the l-th outlet boundary, can be derived from

$$\mathcal{BC}_{1,i}^l = u_i v_j n_j + (\nu + \nu_t) \frac{\partial u_i}{\partial x_j} n_j + (u_j v_j + q) n_i + \frac{\partial F}{\partial v_i}$$

$$+ \underbrace{\tilde{\nu}_a \tilde{\nu} n_i + \tilde{\nu}_a \tilde{\nu} \mathcal{C}_S(\tilde{\nu}) \frac{1}{S} e_{jki} e_{jmq} \frac{\partial v_q}{\partial x_m} n_k}_{termBM1} + \underbrace{T T_a n_i}_{termBM2} + \omega_c \Delta m_l n_i = 0 \tag{17}$$

($i = 1, 2$ in 2D problems; $i = 1, 2, 3$ in 3D problems). Since the number of the unknown quantities in eq. 17 is larger than the number of the available equations by one, a single variable should be zeroed in order to derive the rest of the boundary conditions[5]. In eq. 17, $termBM1$ and $termBM2$ arise from the differentiation of the turbulence model and energy equations, respectively. The last term of the same equation is the sole contribution of the constraint function to the adjoint formulation.

The outlet boundary conditions for the adjoint temperature and the adjoint turbulence variable are given by the Robin type equations $\mathcal{BC}_2 = 0$ and $\mathcal{BC}_3 = 0$, respectively, where

$$\mathcal{BC}_2 \quad = \quad v_i n_i T_a + \left(\frac{\nu}{Pr} + \frac{\nu_t}{Pr_t} \right) \frac{\partial T_a}{\partial x_j} n_j + \frac{\partial F}{\partial T} \tag{18}$$

$$\mathcal{BC}_3 \quad = -\quad \frac{\delta \nu_t}{\delta \tilde{\nu}} u_i \left(\frac{\partial v_i}{\partial x_j} + \frac{\partial v_j}{\partial x_i} \right) n_j - \underbrace{\frac{\delta \nu_t}{\delta \tilde{\nu}} \frac{T_a}{Pr_t} \frac{\partial T}{\partial x_j} n_j}_{termBT1} + \tilde{\nu}_a v_j n_j$$

$$+ \quad \left(\nu + \frac{\tilde{\nu}}{\sigma} \right) \frac{\partial \tilde{\nu}_a}{\partial x_j} n_j + \frac{\partial F}{\partial \tilde{\nu}} \tag{19}$$

In eq. 19, $termBT1$ is present only when heat transfer is included to the adjoint formulation.

At the inlet, Diriclet boundary conditions are imposed to v_i, $\tilde{\nu}$ and T and so, their variations are automatically zeroed. In order to make $\frac{\delta F_{aug}}{\delta \alpha}$ independent of $\frac{\partial p}{\partial \alpha}$, $\frac{\partial}{\partial \alpha} \left(\frac{\partial u_i}{\partial x_j} n_j \right)$, $\frac{\partial}{\partial \alpha} \left(\frac{\partial \tilde{\nu}}{\partial x_j} n_j \right)$, $\frac{\partial}{\partial \alpha} \left(\frac{\partial T_\alpha}{\partial x_j} n_j \right)$, the following inlet adjoint conditions should be imposed

$$u_i n_i = -\frac{\partial F}{\partial p}, \quad u_i t_i = 0 \tag{20}$$

(where t_i are the components of the unit tangent vectors), $\tilde{\nu}_a = 0, T_\alpha = 0$. Since no boundary condition for q results from the elimination of any of the boundary integrals, its normal derivative is set to zero (natural boundary condition).

In a similar way, zero Dirichlet conditions are imposed to u_i, T_a, $\tilde{\nu}_a$ and a zero Neumann to q along the solid wall boundaries.

The adjoint p.d.e.'s with the presented boundary conditions are solved using a scheme equivalent to that of the primal equations, i.e. the adjoint mean–flow equations are solved using the SIMPLE algorithm and, where needed, the adjoint to the heat transfer and turbulence model equations are solved in a decoupled manner.

Finally, the remaining terms of eq. 11 give rise to the sensitivity derivatives of F_{aug} with respect to the variable porosity values

$$\frac{\delta F_{aug}}{\delta \alpha} = \int_\Omega v_i u_i d\Omega + \int_\Omega (T - T_{wall}) T_a d\Omega + \int_\Omega \tilde{\nu} \tilde{\nu}_a d\Omega + \int_\Omega \tilde{\nu}_a \tilde{\nu} \mathcal{C}_d(\tilde{\nu}, \vec{v}) \frac{\partial d}{\partial \alpha} d\Omega \tag{21}$$

So far, the adjoint formulation was general and could be adapted to any objective function. The functions f_i considered in this paper are

$$f_1 \quad = \quad -\int_{S_{I,O}} \left(p + \frac{1}{2} v^2 \right) v_i n_i dS$$

$$f_2 \quad = \quad \int_{S_O} T dS - \int_{S_I} T dS \tag{22}$$

and correspond to the volume–averaged total pressure losses (to be minimized) and the temperature difference between the outlet (S_O) from and the inlet (S_I) to the flow domain (to be maximized), respectively. The norm of the velocity vector is written as v. For the examined heat transfer problems, the objective function (to be minimized) is the weighted sum of f_i i.e. a single scalar function, $F = \omega_1 f_1 - \omega_2 f_2$, where ω_1, ω_2 are user–defined weight factors. The gradient of the objective function F with respect to the state variables

$p, v_i, T, \tilde{\nu}$ is

$$
\begin{aligned}
\frac{\partial F}{\partial p} &= -\omega_1 v_i n_i, \quad \frac{\partial F}{\partial v_i} = -\omega_1 \left(\frac{1}{2} v^2 n_i + v_i v_\lambda n_\lambda + p n_i \right) \\
\frac{\partial F}{\partial \tilde{\nu}} &= 0, \\
\frac{\partial F}{\partial T} &= -\omega_2
\end{aligned}
\tag{23}
$$

3 APPLICATIONS

In this paper, the proposed adjoint method for the solution of topology optimization problems is used to tackle three of them, namely:

- Problem I: the unconstrained optimization of an existing 2D S-bend duct, for a turbulent flow, aiming at minimum viscous losses.

- Problem II: the unconstrained optimization of the topology of a 2D duct with four inlets and four outlets, for a laminar flow, targeting minimum total pressure losses and maximum temperature increase between the inlet and outlet boundaries.

- Problem III: the constrained design of a 3D manifold for predefined volume flow rates at the outlet boundaries and laminar flow conditions, targeting minimum total pressure losses.

Problem I is concerned with the topology optimization of a 2D S-bend duct. The flow is turbulent with Reynolds number, based on the inlet diameter, equal to $Re = 1.2 \times 10^5$. The target is to minimize f_1, so practically $\omega_1 = 1$ and $\omega_2 = 0$. Starting point of the optimization loop is a duct with a large recirculation area; this duct coincides with the porous media domain; see Fig 2, top left. Topology optimization aims at transforming part of the initial flow (i.e. porous media) domain to solid walls, in order to reduce total pressure losses. Fig. 2 shows the velocity field in the recirculation zone before the topology optimization (top–right) and the porosity field calculated at the final step of the optimization algorithm (bottom–left). After post-processing the outcome of the topology optimization, a new duct shape is acquired by interpolating the nodal porosity values to form the new solid wall; the new velocity field can be seen in Fig. 2 (bottom-right). It can be observed that the optimized duct has a reduced recirculation area ($F = 0.16$) and, after 10 optimization cycles, a 15% total pressure loss reduction is achieved, as compared to the initial geometry (for which $F = 0.188$). Numerical experiments have shown that the dominant sensitivity term (eq. 21) is $v_i u_i$. In Fig. 3, light is shed on the mechanism leading to the (partial) elimination of the recirculation areas (and, thus, the minimization of total pressure losses). The angle formed by the primal and adjoint velocities determines the sign of the sensitivity derivative computed at each grid node. Since there is no adjoint (velocity) backflow, areas with negative primal streamwise velocities generate negative sensitivity values (since the inner product becomes locally negative). These sensitivity values lead to an increase of the local porosity variables. Hence, the new solid walls are formed, by eliminating the recirculation areas.

Problem II is dealing with the design of a 2D duct with four inlets and four outlets located along the two opposite sides of a square porous media domain, aiming at minimum total pressure losses and maximum temperature increase. The flow is laminar with $Re = 1000$ based on the width of any of the (equally sized) inlets/outlets. Fig. 4 shows
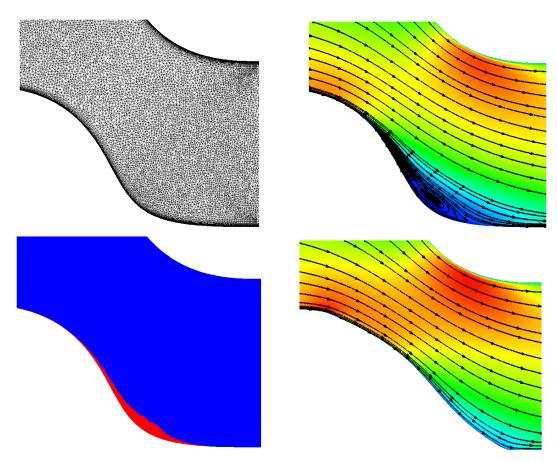
Figure 2: Problem I: Topology optimization of an S-bend duct under turbulent flow conditions, aiming at minimum total pressure losses. Top-left: Unstructured computational grid with 45.700 triangles. Top-right: Velocity field and flow trajectories computed on the initial duct. Bottom-left: Optimal porosity field. Red/bright areas correspond to "new" solid bodies. Bottom-right: Velocity field and flow trajectories of the duct that arises after identifying the new solid wall boundaries, approximating them using a continuous curve and re-solving the flow problem. The reduction of the recirculation area is absolutely clear.
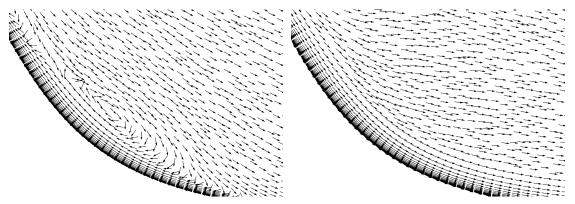

Figure 3: Problem I: Blow–up view of the recirculation area on the lower wall of the initial duct. Primal (left) and adjoint (right) velocity vectors, using uniform vector lengths for visualization purposes. Since $v_i u_i$ (i.e. the inner product of the primal and adjoint velocities) is the dominant term of the sensitivity derivatives, the angle between the primal and adjoint velocity vectors determines the sign of the sensitivities for each grid node. In areas where the primal and adjoint velocities form an obtuse angle, the sensitivity derivatives become negatively signed and this increases the local porosity values. Hence, the recirculation areas tend to disappear.

the flow field and the porous media field, obtained upon completion of the topology optimization. The flow enters the box with fixed temperature ($T_{inlet} = 293K$) and exits it
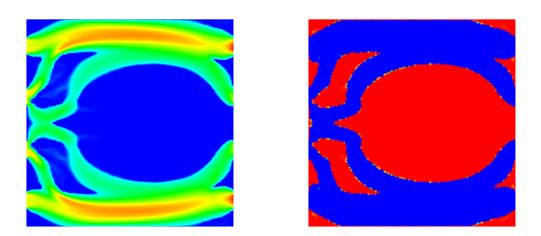
Figure 4: Problem II: Topology optimization of a four inlet/four outlet duct aiming at minimum total pressure losses and maximum increase in fluid temperature. Computations performed over a square porous media domain. Left: Velocity field obtained after the topology optimization loop. Right: Porosity field of the optimal solution. Blue/dark areas depict the flow passage.
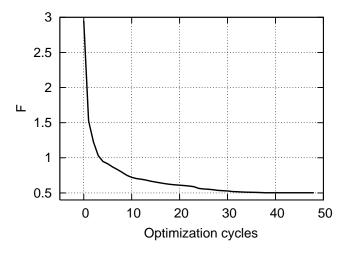

Figure 5: Problem II: Convergence history. Each optimization cycle comprises the solution of the flow and the adjoint equations. F stands for the concatenated objective function with $\omega_1 = 0.7$ and $\omega_2 = 0.3$.

through four predefined openings along its right side. The wall temperature is fixed to $T_{wall} = 353K$. The convergence history of the single scalar objective function F, which concatenates the two objectives by using the user–defined weight factors $\omega_1 = 0.7$ and $\omega_2 = 0.3$, is shown in Fig. 5. In Fig. 4, right, the blue/dark domain, where the porosity is practically zero, represents the flow passage configuration that ensures minimum total pressure losses and maximum increase in fluid temperature. As expected, the flow is preferably developed quite close to the upper and lower hot walls, for the flowing fluid to increase its temperature as much as possible.

Problem III is concerned with the constrained topology optimization of a 3D manifold with one inlet and four outlets; the flow in laminar with $Re = 2000$, based on the inlet hydraulic diameter. Prescribed volume flow rates at each outlet boundary of the porous media domain are imposed as constraints. The target is to minimize total pressure losses.

The incoming flow rate splits by a $20\% - 30\% - 30\% - 20\%$ ratio (of the incoming flow rate) among each of the four outlets. The result of the constrained optimization is compared to the unconstrained one in Fig. 6.
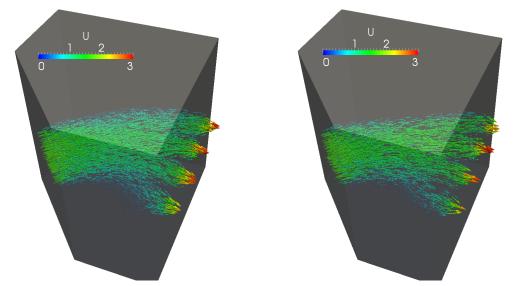

Figure 6: Problem III: Constrained topology optimization of a 3D manifold, targeting at minimum total pressure losses and prescribed volume flow rates at the four outlets. Left: Solution of the unconstrained optimization problem. The flow is almost evenly distributed among the four outlets. Right: Optimal solution of the constrained optimization problem calling for a $20\% - 30\% - 30\% - 20\%$ volume flow rate partition among the four outlets.

4   CONLUSIONS

The continuous adjoint approach to topology optimization problems for laminar and turbulent flows, including heat transfer, was presented. The heat transfer and turbulence model equations were enriched with new porosity dependent terms in order to formulate the topology optimization problem. For turbulent flows, the adjoint formulation was presented without making the "usual" assumption that variations in topology do not affect turbulence; extra terms and equations resulting from the differentiation of the Spalart-Allmaras turbulence model were considered in the present formulation. Constraints regarding desirable volume flow rates at each flow outlet were formulated and included in the adjoint-based optimization.

5   ACKNOWLEDGEMENTS

REFERENCES

[1] Bendsoe, M., Kikuchi, N. Generating optimal topologies in structural design using a homogenization method. *Journal of Computer Methods in Applied Mechanics and Engineering.* **71**, 197-224 (1988).

[2] Guest, J., Prevost, J. Topology optimization of creeping fluid flows using a Darcy–Stokes finite element. *International Journal for Numerical Methods in Engineering.* **66**, 461–484 (2006).

[3] Gersborg-Hansen, A., Sigmund, O., Haber, R. Topology optimization of channel flow problems. *Structural and Multidisciplinary Optimization.* **30**, 181–192 (2005).

[4] Othmer, C. A continuous adjoint formulation for the computation of topological and surface sensitivities of ducted flows. *International Journal for Numerical Methods in Fluids.* **58**(8), 861-877 (2008).

[5] Zymaris, A.S., Papadimitriou, D.I., Giannakoglou, K.C., Othmer, C. Continuous Adjoint Approach to the Spalart Allmaras Turbulence Model, for Incompressible Flows. *Computers & Fluids.* **38** 1528-1538 (2009).

[6] Spalart, P., Allmaras, S. A one–equation turbulence model for aerodynamic flows. *La Recherche Aerospatiale.* **1** 5–21(1994).

[7] Careto, L.S., Gisman, A.D., Patankar, S.V., Spalding, D.B. Two calculation procedures for steady three-dimensional flows with recirculation. *Proceedings of the Third International Conference on Numerical Methods in Fluid Mechanics*, Paris (1972).